© 2020. Published by The Company of Biologists Ltd | Journal of Experimental Biology (2020) 223, jeb208678. doi:10.1242/jeb.208678

SHORT COMMUNICATION

Medium compensation in a spring-actuated system

Kathryn D. Feller[1,*,‡], Gregory P. Sutton[2] and Paloma T. Gonzalez-Bellido[3]

ABSTRACT

Mantis shrimp strikes are one of the fastest animal movements, despite their occurrence in a water medium with viscous drag. Since the strike is produced by a latch-mediated spring-actuated system and not directly driven by muscle action, we predicted that strikes performed in air would be faster than underwater as a result of reduction in the medium's drag. Using high-speed video analysis of stereotyped strikes elicited from *Squilla mantis*, we found the exact opposite: strikes are much slower and less powerful in air than in water. *S. mantis* strikes in air have a similar mass and performance to latch-mediated spring-actuated jumps in locusts, suggesting a potential threshold for the energetics of a 1–2 g limb rotating in air. Drag forces induced by the media may be a key feature in the evolution of mantis shrimp strikes and provide a potential target for probing the braking system of these extremely fast movements.

KEY WORDS: Biomechanics, Energy, Kinematics, Power amplification, Stomatopod

INTRODUCTION

Diverse biological systems, including locusts and mantis shrimp, use latch-mediated, spring-actuated systems to generate movements with incredibly high speeds and mechanical power (Gronenberg, 1996; Ilton et al., 2018; Patek et al., 2011; Rosario and Patek, 2015). The speeds of these systems are often so fast that neural feedback is insufficient to change the behavior once the loaded spring is released. The 1–2 ms timeframe of these movements necessitates use of open-loop neural control to set the speed and direction of the behavior prior to de-latching the spring (Burrows, 2006; Kagaya and Patek, 2016; Patek et al., 2006). Mantis shrimp (stomatopods), in particular are known for their ability to propel a specialized pair of spring-actuated maxillipeds (raptorial appendages) at speeds of up to 30.6 m s^{-1} (Cox et al., 2014). The strike is used for multiple behaviors including predation, agonistic combat and defense, and its output force can be tuned according to these different tasks (Green et al., 2019). Like other spring-actuated biological systems, in mantis shrimp the movement is preceded by first latching the raptorial appendages in place before co-contracting large muscles that store potential energy in spring-like, cuticular structures (Rosario and Patek, 2015). When the latch disengages, the spring releases, converting the stored energy into rotational movement of the striking appendages (Fig. 1). In other systems with spring-actuated movements (such as locusts, froghoppers and fleas), elastic energy is completely transmitted to kinetic energy (Bennet-Clark, 1975). Given that mantis shrimp use similar mechanics to other spring-actuated systems, we hypothesized that the same amount of energy would be stored prior to strikes deployed for a single behavioral task. A fundamental difference between mantis shrimp strikes and other systems, however, is that mantis shrimp strike in water rather than in air. By measuring the speed of strikes in air and in water, our hypothesis predicts that strikes in air (not slowed down by viscous water drag) will be faster than those in water. Unexpectedly, the exact opposite was observed.

MATERIALS AND METHODS

Animals and high speed video recording

Live, healthy mantis shrimp of the species *Squilla mantis* (Linnaeus 1758) were purchased from local fishermen in Andalucia, Spain in January 2018. Animals were captured using traditional fishing methods and maintained in a large bucket of seawater until purchase, then transported to Málaga, Spain and housed in filtered seawater aquaria. All experiments were conducted within 1–2 days of collection on six females and one male, all from the same collection.

Lightly restrained mantis shrimp were held in a fixed position and mechanically stimulated to strike in air, then in water (or the reverse) by adjusting the water level in the aquarium. Neither animal nor camera were moved between treatments. High-speed video (HSV) cameras (5000 frames s^{-1}, 1024×640 pixel resolution, Photron SA2 model 86K-M4, San Diego, CA, USA) were positioned lateral to the animal to record strikes. Approximately 2.5 cm of space lay between the animal and the aquarium glass, minimizing magnification effects of the image from the addition of water. Videos were captured and saved using Photron FastCam Visualization software (v.3.6.9.0) run on a PC laptop (Gigabyte P34 Geforce GTX 1050). Only strikes generated by the appendage ipsilateral to the camera were analyzed. The order by which each animal experienced different media was randomized among the seven individuals tested. A minimum of five strikes were recorded per animal in each medium condition (water or air), although only strikes that exhibited the initial sliding motion of the carpus (Fig. S1) – indicating release of the latch mechanism – were analyzed (Patek et al., 2007). One animal was tested in water, then air, then back to water because of its robust participation in the experiment. This was also the only male tested.

Each individual was mounted on a gimballed platform (Nootle, Grifiti LLC, Sausalito, CA, USA), ventral surface up (supine position). A partial restraint was developed to control for variation in body posture between strikes induced in different media (air and water). In a restrained prone position, the raptorial appendages passively open under gravity. Supine restraint allowed the raptorial appendages to remain in a consistent, folded position. Padded, plastic-coated wire restraints were used to fix the animal to the gimballed platform at two points: the first pair of walking legs and

[1]Department of Physiology Development and Neuroscience, University of Cambridge, Cambridge CB2 3EG, UK. [2]University of Lincoln, School of Life Sciences, Lincoln LN6 7TS, UK. [3]Ecology Evolution and Behavior Department, University of Minnesota, St Paul, MN 55108, USA.
*Present address: Ecology Evolution and Behavior Department, University of Minnesota, St Paul, MN 55108, USA.

‡Author for correspondence (kate.feller@gmail.com)

K.D.F., 0000-0003-4730-2105; G.P.S., 0000-0002-3099-9842

Received 17 June 2019; Accepted 16 January 2020

Journal of Experimental Biology (2020) 223, jeb208678. doi:10.1242/jeb.208678

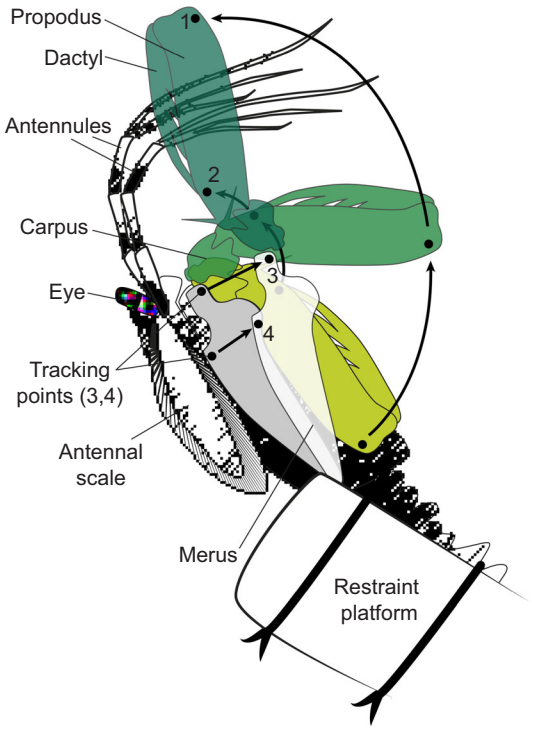

Fig. 1. Experimental setup to measure kinematics of closed dactyl defensive strikes in *Squilla mantis*. Numbered dots 1–4 represent tracking points used to define two vectors, from which angular velocity was calculated (as in Kagaya and Patek, 2016). Tracking points are also depicted in photograph of *S. mantis* in Fig. S1D.

the telson. This restraint only restricted movement in the posterior abdomen, leaving the thoracic carapace and maxillapeds free. The restraints were also placed outside the range of the pleopods, so fanning and respiration could occur. The gimballed platform was adjusted to ∼45 deg angle to allow the pleopods to remain submerged. The mounted animal was placed in a small (∼20 liter) aquarium containing enough seawater to cover the abdomen and gills (air treatment) or completely submerge the animal (water treatment). Strikes were elicited by mechanical stimulation to the abdomen with a 4-mm-diameter fiberglass stick, eliciting reproducible, defensive-type strike responses. All animals were in good health upon completing the experiment.

Strike kinematic analyses and statistics

Strike videos were saved in Tiff stack format and opened in ImageJ (Fiji; Schindelin et al., 2012). Using the ImageJ plugin MTrackJ (Meijering et al., 2012), two points on the propodus and two points on the merus were manually tracked using natural landmarks and/or a small piece of black nylon glued to the appendage. The change in angle between the two lines described by points 1–2 and 3–4 (Fig. 1) was used to calculate the angular velocity of the rotating appendage during each strike using R code modified from the literature (Kagaya and Patek, 2016; McHenry et al., 2016). A polynomial function of 10 was fit to the resulting angular rotation data over time. Angular velocity was calculated as the first derivative of the smoothed rotation curve. Angular acceleration was calculated as the second derivative of angular rotation as a function of time. Movement of the carpus during a strike was measured as a function of linear distance over time between two points digitized on the merus and carpus (Fig. S1A–D). Start times for both carpus slide and propodus rotation were quantified as time of peak acceleration for each movement. The difference between the start time of propodus rotation and carpus slide was then calculated as a metric (C_T) to quantify carpus sliding (Fig. SA–C).

As animals survived beyond the experiment, the exact masses of each segment of the raptorial appendage could not be measured. Instead, masses of the merus, propodus and dactyl were estimated from mass and dimensional data compiled from additional *S. mantis* specimens. Morphometric measurements of limb features and the total wet mass of each measured limb segment were collected from 12 individuals additional to those recorded in the strike experiment. Each limb segment mass was plotted vs the dimensional measurements and fit to a linear regression (R^2>8.3; Fig. S1). The morphometric dimensions were selected based on their lateral visibility in video recordings of mantis shrimp strikes. The raptorial limb dimensions of individuals used in the strike experiment were then measured using calibrated still frames from the high-speed video data. These measurements were used to estimate mass via the linear regression equations (reported in Fig. S1). Due to differences in merus size, a metric of meral width multiplied by meral saddle width was used to evaluate mass.

Energy and power were calculated by modelling the propodus and dactyl as rigid bodies rotating about the proximal end of the propodus. The energy in the propodus was:

$$E_{\text{propodus}} = \frac{1}{2}\left(\frac{1}{3} m_{\text{p}}\, l_{\text{p}}^2\right)\dot{\theta}^2, \quad (1)$$

where m_{p} is the mass of the propodus in kg, l_{p} is the length of the propodus in m, and $\dot{\theta}$ is the angular velocity of the limb (dactyl and propodus) in rad s^{-1}. The dactyl, which was modelled as a rigid body attached at the distal end of the propodus (Fig. 1), is also rotating about the proximal end of the propodus. Because the dactyl attaches at the distal end of the propodus, the parallel axis theorem must be used to calculate its kinetic energy, thus causing its kinetic energy to be:

$$E_{\text{dactyl}} = \frac{1}{2}\left(\frac{1}{3} m_{\text{d}} l_{\text{p}}^2 + m_{\text{d}} \times (l_{\text{p}} - l_{\text{d}})^2\right)\dot{\theta}^2, \quad (2)$$

where m_{d} is the mass of the dactyl in kg, l_{d} is the length of the dactyl in m, and $\dot{\theta}$ is the angular velocity of the limb (dactyl and propodus) in rad s^{-1}. The total energy was the sum of the kinetic energy in the propodus and the kinetic energy in the dactyl.

Power was calculated by dividing the peak kinetic energy during the strike by the time between the initial movement of the propodus and the time of peak angular rotation (the acceleration time). The time between the initial motion and the moment that the propodus reached its highest angular velocity is thus the 'launch' time for this latch-mediated spring-actuated system (Longo et al., 2019). Paired *t*-test statistical analyses were performed in R to assess the mean differences in strikes performed in air vs water (n=7).

RESULTS AND DISCUSSION

A total of 31 strikes in air and 36 strikes in water were recorded and analyzed from seven animals, with individual energetic parameters being estimated by generating a mean for each individual animal, and then the means of the seven animals calculated here. The number of air and water strikes measured by individual and their associated kinematics are reported in Table S1. The majority of the specimens were female (six) with only one male represented, owing to random collection of specimens.

Journal of Experimental Biology (2020) 223, jeb208678. doi:10.1242/jeb.208678

Table 1. Kinematics of strikes from *Squilla mantis*

	No. of strikes	Angular velocity (deg s^{-1})	Acceleration time [launch] (ms)	Decceleration time [after launch] (ms)	Kinetic energy (mJ)	Power (W)	Tip velocity (m s^{-1})
Air strikes							
Animal 1	3	6200	9.1	9.3	4.9	0.54	4.5
Animal 2	2	10,240	9.2	10	7.5	0.82	6.3
Animal 3	4	7910	14.6	15.6	4.5	0.31	4.7
Animal 4	3	5770	21	7	2.3	0.11	3.5
Animal 5	5	8280	18.9	14.2	3.4	0.18	4.9
Animal 6	4	8080	13.7	18	3.3	0.24	4.6
Animal 7	10	11,250	12.7	14.7	9.0	0.70	6.7
Mean±s.d.	–	8250±1980	14.2±4.5	14.2±4.5	5.0±2.4	0.42±0.28	5.0±1.1
Water strikes							
Animal 1	2	14,780	7.6	10.3	28.0	3.7	10.7
Animal 2	3	15,530	7.3	11.7	17.4	2.4	9.6
Animal 3	6	17,830	7.7	8.3	23.0	3.0	10.6
Animal 4	5	10,056	9.9	13.4	7.1	0.7	6.1
Animal 5	4	10,110	9.4	9.5	5.1	0.5	6.0
Animal 6	6	19,380	8.6	7.7	19.0	2.2	11.0
Animal 7	10	11,292	7.9	15.6	9.0	1.2	6.7
Mean±s.d.	–	14,140±3750	8.3±1.0	10.9±2.8	15.5±8.6	2.0±1.2	8.7±1.3

When striking in air, *S. mantis* propels its limb with a mean peak angular velocity of 8250±1980 deg s^{-1} (tip velocity 5.0±1.1 m s^{-1}; Table 1, Fig. 2B). When striking in water, the rotating limb is propelled almost twice as quickly 14,140±3750 deg s^{-1} (tip velocity 8.7±1.3 m s^{-1}; Table 1, Fig. 2C). Water strikes therefore have three times more kinetic energy than air strikes (15.5±8.6 mJ vs 5.0±2.4 mJ in water vs air) and almost five times the power (2.0±1.2 W vs 0.42±0.28 W in water vs air) (Table 1, Fig. 2D–G). No evidence of fatigue effect (such as decreased strike velocity) was observed among sequential strikes performed by any individual (Fig. 2A). Paired *t*-tests revealed significant differences between air and water strike velocity (P=1.1e−04) and acceleration (P=1.5e−07). Significant differences in power were observed during the strike launch (initiation of movement to the moment of peak velocity, corresponding to spring actuation; P=2.2e−02). Although takeoff power (time from peak velocity to the end of the strike, corresponding to movement not actuated by the spring) presents a similar trend to launch power, the difference was not significant in this dataset (P=7.9e−02; Fig. 2H).

The power per muscle mass of water strikes (1144±604 W kg^{-1}, N=7; range=364–1936) indicated that *S. mantis* use an elastic storage system since these values exceed the power output limit of high power muscle (~400 W kg^{-1}, Askew and Marsh, 2002). Air strikes, however, yielded significantly less power, suggesting that an elastic storage system may not be used during these strikes. However, we cannot rule out the use of elastic storage during air strikes for several reasons. First, two of the animals had air strikes with power outputs higher than 400 W kg^{-1} (485 and 414 W kg^{-1}), indicating that elastic storage was utilized at least twice. Second, our method of evaluating elastic storage overestimated extensor muscle mass (used total limb segment mass) and ignored energy losses to the medium (i.e. underestimated the energy, and thus power density during movement). Third, unlike the very ‘fast’ muscles used to define the 400 W kg^{-1} limit, the extensor muscles in the merus are not particularly ‘fast’ and can take as long as 700 ms to reach maximum tension (Burrows and Hoyle, 1972; Patek, 2019). This means that the power threshold for *S. mantis* muscles alone is likely to be much less than 400 W kg^{-1}. Finally, carpus sliding prior to strike rotation is an accepted metric for reporting deployment of an elastic mechanism (Patek et al., 2007). Our quantification of the carpus slide revealed that 100% of strikes analyzed present a carpus movement initiated prior to strike (7.6±5.1 ms). The carpus sliding movement occurs significantly faster during the fastest strikes (>15,000 deg s^{-1}) than the slowest strikes (<8000 deg s^{-1}; P=3.1e−04; Fig. S1C).

If we assume that *S. mantis* utilized a latch-mediated spring-actuated strike in both air and water strikes, these results can be explained by two possible mechanisms. Either, the force of the mechanical strike system does not transfer as efficiently in air as it does in water, or mantis shrimp modulate the speed of their strike based on the surrounding medium. Given recent findings related to strike modulation in different behavioral contexts (Green et al., 2019), and the current hypothesis as to how this system functions (Rosario and Patek, 2015), it is unclear to us how a difference in medium would change the transmission of energy from elastic structures in the appendage into kinetic energy. Consequently, the latter hypothesis, that the strike speed is modulated, is a much more likely explanation of our findings.

A second result of our experiment is an observed coincidence between the amount of energy *S. mantis* air strikes produced and the grasshopper latch-mediated spring-actuated jump system. When striking in air, the mantis shrimp accelerates a 1.2±0.21 g limb with a mechanical power output of 0.42±0.28 W, despite the fact that the *S. mantis* is mechanically capable of generating up to almost 4 W of power (Table 1). The power output of the mantis shrimp, (0.42±0.28 W) is similar to the power output of the similarly sized jumping adult grasshopper, which accelerates 1.5–2.0 g of mass with 0.3–0.8 W of mechanical energy (Bennet-Clark, 1975). Likewise, the kinetic energy output of the mantis shrimp (5.0±2.4 mJ; Table 1) is also similar to that of a single locust leg (4.5–5.5 mJ, (Bennet-Clark, 1975). The similar performances of these evolutionarily divergent systems suggests that there may be a maximum kinetic energy capacity limit for 1–2 g airborne latch-mediated, spring-actuated biological systems. That the mantis shrimp performs strikes at this limit in air, even though it is mechanically able to strike much faster, suggests a hypothesis that faster movements, without media to dissipate excess kinetic energy, may damage the system. Evaluation of other similarly sized latch-mediated spring-actuated systems need to be analyzed to differentiate between this hypothesis or the alternative – that this is just a coincidence.

Journal of Experimental Biology (2020) 223, jeb208678. doi:10.1242/jeb.208678

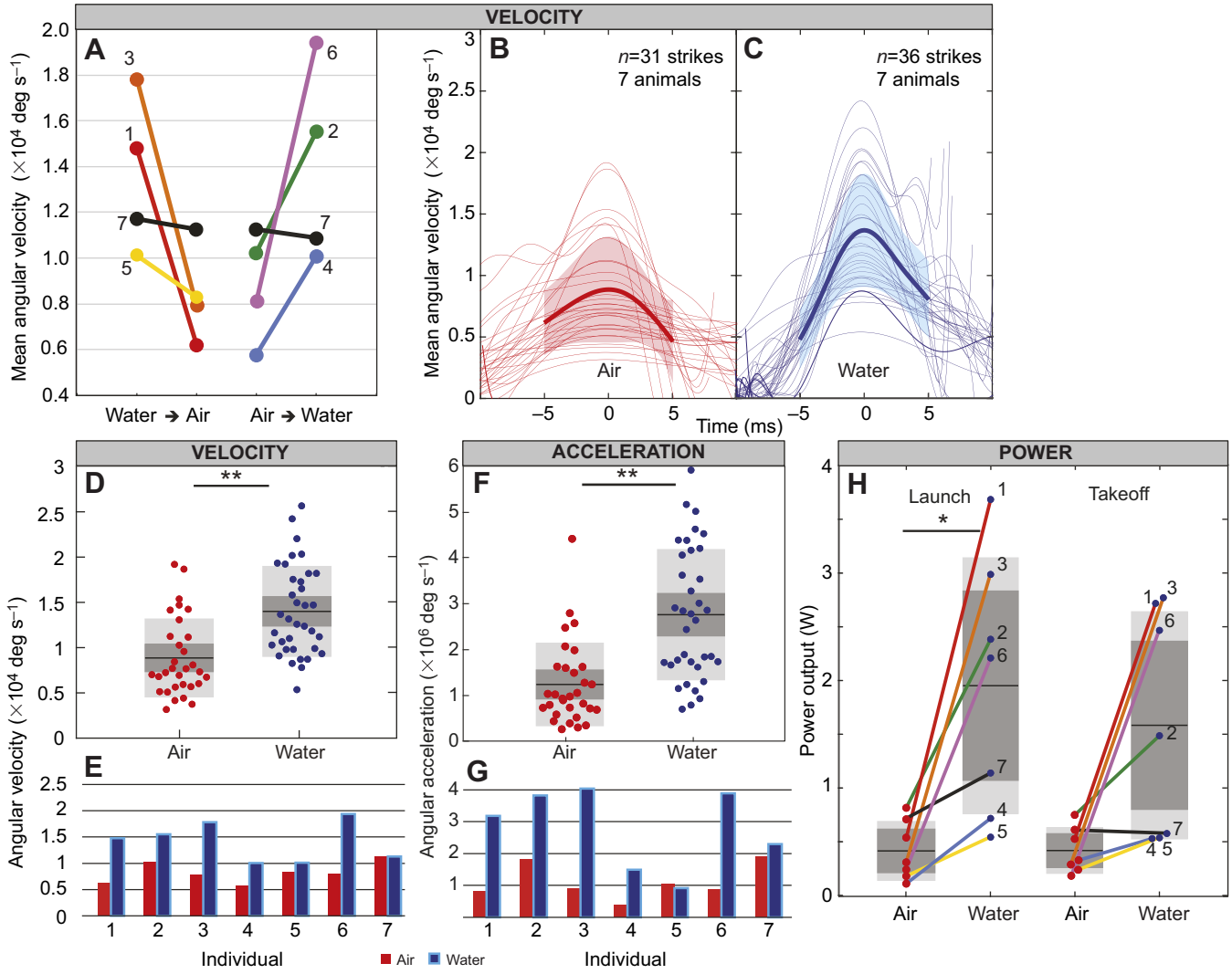

Fig. 2. Kinematics of air versus water strikes performed by *S. mantis*. (A) Mean angular velocity of strikes from each individual trial experienced either in water then in air, or the reverse. Numbers indicate individual measured. Animal 7 (black), the token male available during the experiment, was measured in both transitions. (B,C) Angular velocity over time of individual strikes from all animals in air (B) and water (C). Thick red or blue lines and shaded areas surrounding each line represent mean velocity and s.d., respectively. Mean calculations were truncated at ±5 ms from peak for analysis purposes. (D) Plot of raw, peak angular velocity data from all air (red) and water (blue) strikes. Plots show raw data (dots), mean (black horizontal line), 1.96 s.e.m.(dark grey shading) and s.d. (light grey shading). (E) Mean air and water angular velocity by individual. (F) Peak angular acceleration of all strikes. (G) Mean air and water strike angular acceleration by individual. (H) Mean power calculated by individual for the launch and takeoff periods of the strike. Lines and numbers correspond to individual animals in A. F and H show the same format for data, mean, s.e.m. and s.d. presentation as described in D. Paired *t*-test significant groups, **P*<0.05; ***P*<0.001.

One of the most remarkable features of biological spring-actuated systems is their ability to load, release and dissipate large amounts of energy such that the system can be used again and again without incurring damage. The huge amount of energy released from a recoiling spring system creates the need for systems to help control the limb and absorb excess kinetic energy. An appropriate limb 'set up' minimizes possible errors and prevents damage to the system prior to the initiation of the behavior. In the previously discussed locust leg system, use of the shock-absorbing material resilin serves to spill off any unused kinetic energy when the joint reaches its maximum angle (Bayley et al., 2012). Although mantis shrimp produce one of the fastest spring-actuated movements, the braking mechanism is not currently known. Studies of drag for species with similarly sized raptorial appendages (*Lysiosquillina maculata*), estimate that the water can absorb 10–20 mJ of energy during a strike (McHenry et al., 2016), predicting that the medium absorbs most of the kinetic energy during a strike in water. Since a shock absorbing mechanism analogous to the locust limb is not known in mantis shrimp raptorial appendages, it is possible that, in air, mantis shrimp may prevent damage to the joint by simply striking more slowly. The similar energetics of stomatopod and locust spring-actuated movements in air provide a good paradigm for investigating properties of the mantis shrimp limb that dissipate residual energy in the absence of both resilin and viscous drag.

In conclusion, we show that the surrounding medium affects output forces generated during mantis shrimp strikes. Our findings contribute to growing evidence that mantis shrimp precisely control strike output behaviors, despite their 'feed forward' control. To control such behaviors, an assembly of information from both the external environment and internal muscular state must be processed to predict the consequences of a strike prior to execution. In both the air and water strikes, the animals struck at open space in response to

posterior prodding. Defensive strikes executed from freely moving *S. mantis* individuals perturbed anteriorly with a stick, might be even faster than defensive water strikes from restrained individuals. Mantis shrimp may engage faster, more powerful strikes when they receive sensory feedback that describes both sufficient medium viscosity and an impact target to absorb excess strike energy. We subsequently propose the hypothesis that the surrounding medium and strike target work together as external shock absorbers for mantis shrimp strikes. As research moves forward to characterize the mechanisms underlying strike brakes and power output modulations, the properties of the surrounding medium should also be considered.

Acknowledgements
We thank Margarita Paloma Bellido Martin and Enrique Gonzalez Silva for their generous help in the field; Jacob Harrison for answering questions pertaining to analysis; as well as Sheila Patek and Malcolm Burrows for feedback and discussion.

Competing interests
The authors declare no competing or financial interests.

Author contributions
Conceptualization: K.D.F., G.P.S., P.T.G.-B.; Methodology: K.D.F., G.P.S.; Software: K.D.F.; Validation: K.D.F.; Formal analysis: K.D.F., G.P.S.; Investigation: K.D.F.; Resources: K.D.F., P.T.G.-B.; Data curation: K.D.F.; Writing - original draft: K.D.F., G.P.S.; Writing - review & editing: K.D.F., G.P.S., P.T.G.-B.; Visualization: K.D.F.; Supervision: P.T.G.-B.; Project administration: K.D.F.; Funding acquisition: K.D.F., P.T.G.-B.

Funding
This work and K.D.F. were supported by a Marie Sklodowska-Curie Independent Postdoctoral Research Fellowship distributed by the European Commission, MSCA-IF Project: EYEPOD 702238. K.D.F. was also supported by funding from the University of Minnesota College of Biological Sciences.

Supplementary information
Supplementary information available online at
http://jeb.biologists.org/lookup/doi/10.1242/jeb.208678.supplemental

References
Askew, G. N. and Marsh, R. L. (2002). Muscle designed for maximum short-term power output: quail flight muscle. *J. Exp. Biol.* **205**, 2153-2160.
Bayley, T. G., Sutton, G. P. and Burrows, M. (2012). A buckling region in locust hindlegs contains resilin and absorbs energy when jumping or kicking goes wrong. *J. Exp. Biol.* **215**, 1151-1161. doi:10.1242/jeb.068080
Bennet-Clark, H. C. (1975). The energetics of the jump of the locust Schistocerca gregaria. *J. Exp. Biol.* **63**, 53-83.
Burrows, M. (2006). Jumping performance of froghopper insects. *J. Exp. Biol.* **209**, 4607-4621. doi:10.1242/jeb.02539
Burrows, M. and Hoyle, G. (1972). Neuromuscular physiology of the strike mechanism of the mantis shrimp, Hemisquilla. *J. Exp. Zool.* **179**, 379-393. doi:10.1002/jez.1401790309
Cox, S. M., Schmidt, D., Modarres-Sadeghi, Y. and Patek, S. N. (2014). A physical model of the extreme mantis shrimp strike: kinematics and cavitation of Ninjabot. *Bioinspir. Biomim.* **9**, 016014. doi:10.1088/1748-3182/9/1/016014
Green, P. A., McHenry, M. J. and Patek, S. N. (2019). Context-dependent scaling of kinematics and energetics during contests and feeding in mantis shrimp. *J. Exp. Biol.* **222**, jeb198085. doi:10.1242/jeb.198085
Gronenberg, W. (1996). Fast actions in small animals: springs and click mechanisms. *J. Comp. Physiol. A* **178**, 727-734. doi:10.1007/BF00225821
Ilton, M., Bhamla, M. S., Ma, X., Cox, S. M., Fitchett, L. L., Kim, Y., Koh, J.-S., Krishnamurthy, D., Kuo, C.-Y., Temel, F. Z. et al. (2018). The principles of cascading power limits in small, fast biological and engineered systems. *Science* **360**, eaao1082. doi:10.1126/science.aao1082
Kagaya, K. Patek, S. N. (2016). Feed-forward motor control of ultrafast, ballistic movements. *J. Exp. Biol.* **219**, 319-333. doi:10.1242/jeb.130518
Longo, S. J., Cox, S. M., Azizi, E., Ilton, M., Olberding, J. P., St Pierre, R. and Patek, S. N. (2019). Beyond power amplification: latch-mediated spring actuation is an emerging framework for the study of diverse elastic systems. *J. Exp. Biol.* **222**, jeb197889. doi:10.1242/jeb.197889
McHenry, M. J., Anderson, P. S. L., Van Wassenbergh, S., Matthews, D. G., Summers, A. P. and Patek, S. N. (2016). The comparative hydrodynamics of rapid rotation by predatory appendages. *J. Exp. Biol.* **219**, 3399-3411. doi:10.1242/jeb.140590
Meijering, E., Dzyubachyk, O. and Smal, I. (2012). Methods for cell and particle tracking. *Methods Enzymol.* **504**, 183-200. doi:10.1016/B978-0-12-391857-4.00009-4
Patek, S. N. (2019). The power of mantis shrimp strikes: interdisciplinary impacts of an extreme cascade of energy release. *Integr. Comp. Biol.* **59**, 1573-1585. doi:10.1093/icb/icz127
Patek, S. N., Baio, J. E., Fisher, B. L. and Suarez, A. V. (2006). Multifunctionality and mechanical origins: ballistic jaw propulsion in trap-jaw ants. *Proc. Natl. Acad. Sci. USA* **103**, 12787-12792. doi:10.1073/pnas.0604290103
Patek, S. N., Nowroozi, B. N., Baio, J. E., Caldwell, R. L. and Summers, A. P. (2007). Linkage mechanics and power amplification of the mantis shrimp's strike. *J. Exp. Biol.* **210**, 3677-3688. doi:10.1242/jeb.006486
Patek, S. N., Dudek, D. M. and Rosario, M. V. (2011). From bouncy legs to poisoned arrows: elastic movements in invertebrates. *J. Exp. Biol.* **214**, 1973-1980. doi:10.1242/jeb.038596
Rosario, M. V. and Patek, S. N. (2015). Multilevel analysis of elastic morphology: the mantis shrimp's spring. *J. Morphol.* **276**, 1123-1135. doi:10.1002/jmor.20398
Schindelin, J., Arganda-Carreras, I., Frise, E., Kaynig, V., Longair, M., Pietzsch, T., Preibisch, S., Rueden, C., Saalfeld, S., Schmid, B. et al. (2012). Fiji: an open-source platform for biological-image analysis. *Nat. Methods* **9**, 676-682. doi:10.1038/nmeth.2019

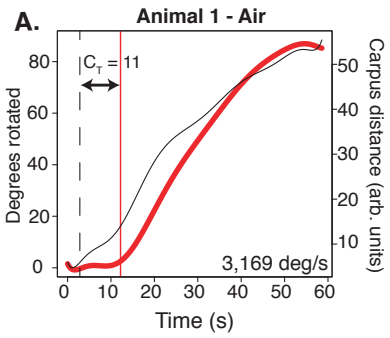

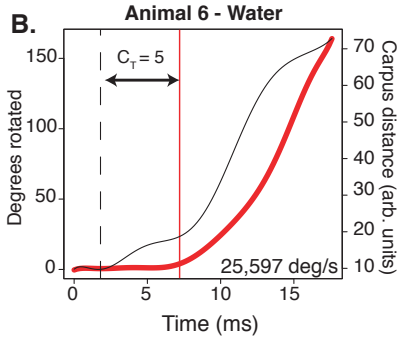

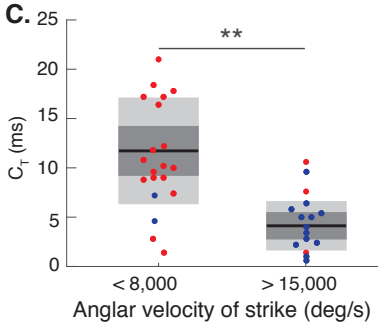

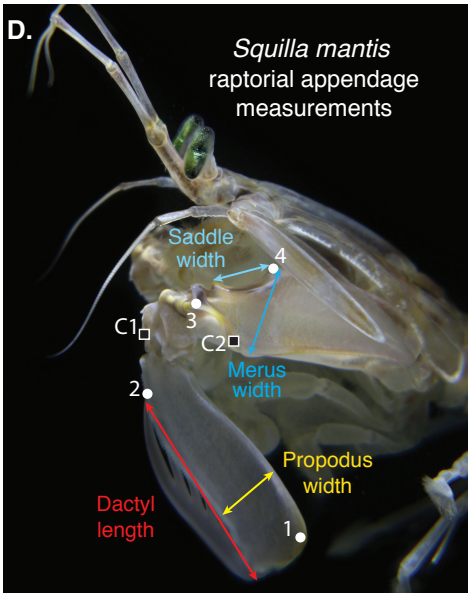

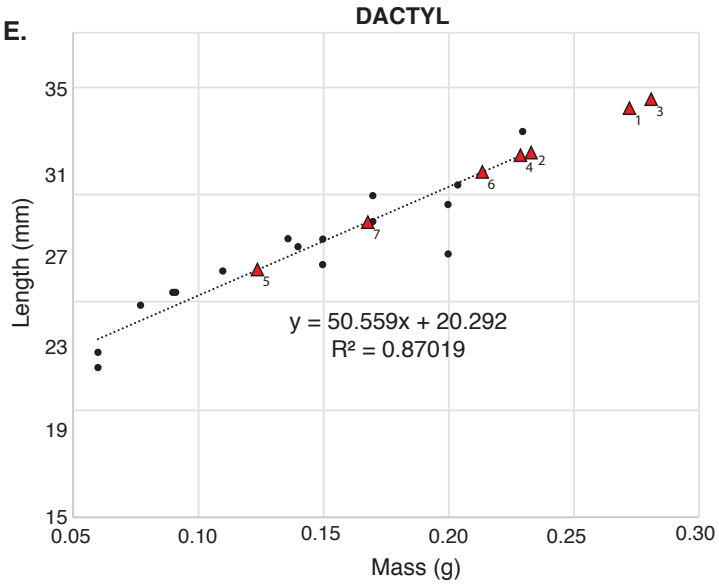

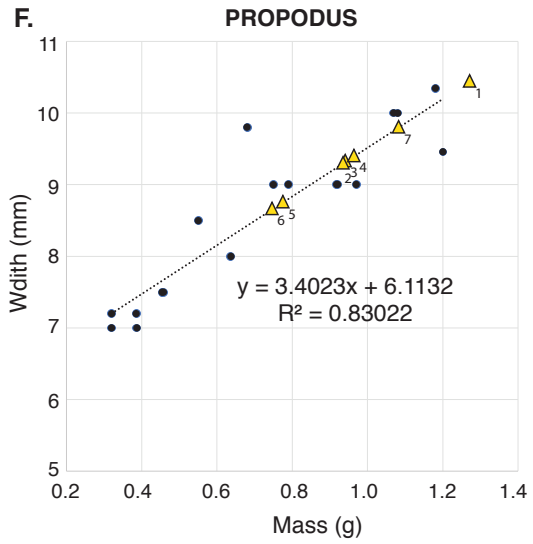

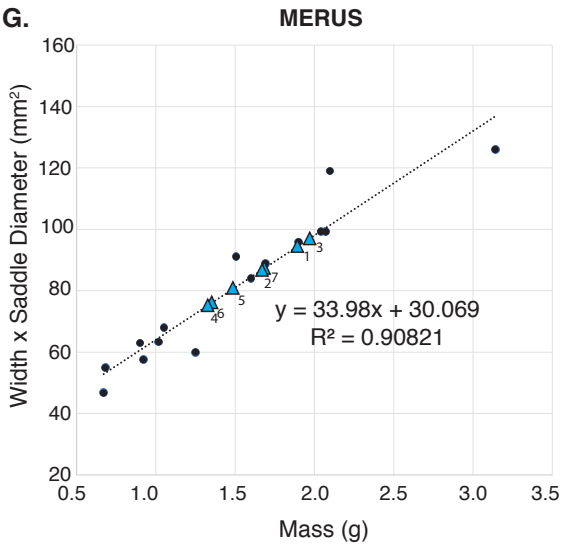

Journal of Experimental Biology • Supplementary information

Figure S1. Morphometric analyses of *S. mantis* to assess carpus sliding during strike and raptorial appendage segments used to estimate mass. **A.** The change in angular rotation (red trace, smooth data with polynomial 10 function) of a slow air and a **B.** fast water strike vs. carpus sliding during a strike (black line). C_T is the time (in ms) from initiation of carpus movement away from merus (vertical dashed line) to the time propodus rotation is initiated (red vertical line). Value in lower right corner of A and B traces is peak angular velociety (deg/s) of strike. **C.** C_T times measured from strikes with peak velocities less than 8000 deg/s and greater than 15,000 deg/s. **D.** Photograph of *S. mantis* depicting digitization points for calculating angular rotation (white circles 1-4), carpus sliding (black squares C1-C2), and locations of measurements collected from raptorial appendage segments used to estimate mass. **E.** Relationship of dactyl length measurement to dactyl mass. **F.** Propodus width vs. mass. **G.** Metric value of merus width multiplied times saddle width vs. meral mass. Black circles, mass and morphometric data collected from 15 fresh raptorial appendages from 12 animals not used in air/water experiment; triangles, morphometric values of raptorial appendage segments from each individual evaluated in air/water strike experiment. Subscript numbers represent individual numbering reported in Fig 1B. Colors in B-D correspond to segment measurements in A: red, dactyl; yellow, propodus; blue, merus. ; paired T-test significant groups: **, p-value < .001.

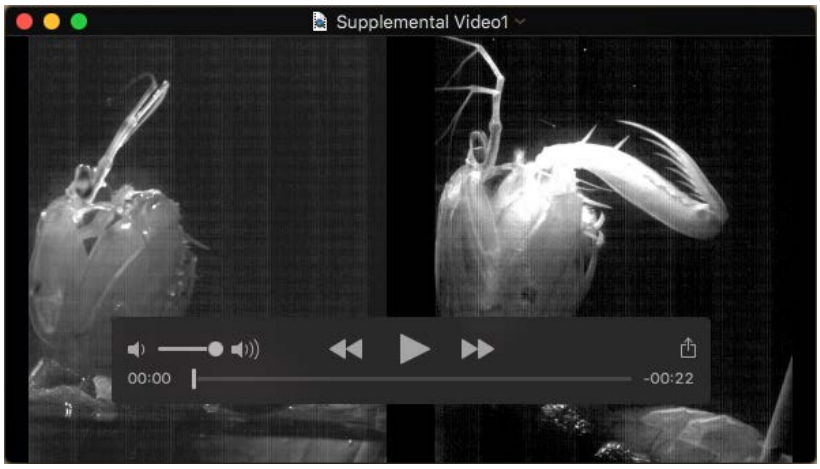

Movie 1. *S. mantis* induced to strike in water and in air. Notice how the lack of stability in the merus-propodus joint in air

Journal of Experimental Biology • Supplementary information

Table S1: Raptorial Limb Morphology and estimated masses in *Squilla mantis*

Animal	Propodus				Dactyl		
	Mass (g)	**Length (mm)**	**Inertia (g.mm.mm)**		**Mass (g)**	**Length (mm)**	**Inertia (g.mm.mm)**
1	1.27	41.3	722		0.27	34	118
2	0.93	35.5	391		0.23	32.1	82
3	0.94	34.1	364		0.28	34.5	111
4	0.96	34.5	381		0.23	31.9	80
5	0.77	33.9	295		0.12	26.5	35
6	0.75	32.5	264		0.21	31.1	68
7	1.08	33.9	414		0.17	28.8	51
Mean	0.96	35.1	404		0.22	31.3	78
S.D.	0.18	2.9	150		0.06	2.8	30

Journal of Experimental Biology • Supplementary information